RARE METALS
Vol. 30, No. 5, Oct 2011, p. 550
DOI: 10.1007/s12598-011-0428-9

Mechanical properties and fracture behaviors on 6061 aluminum alloy under shear stress state

ZHU Hao and QI Fangjuan

College of Materials Science and Engineering, Shijiazhuang Tiedao University, Shijiazhuang 050043, China

Received 10 November 2010; received in revised form 18 April 2011; accepted 20 April 2011

Abstract

The mechanical properties and fracture behaviors of 6061 aluminum alloy were investigated by the tensile shear tests and *in-situ* tensile shear tests with tensile shear specimen devised. The results indicate that many slip bands parallel to tensile direction are produced on the surfaces of the specimens. With shear strain rates increasing, the shear yield stress and shear ultimate stress of 6061 aluminum alloy remain constant basically, but the shear fracture strain decreases obviously. The shear strain rates have no influence on the fracture surfaces. The grain boundaries of 6061 aluminum alloy are the weakest area and microcracks initiate at the grain boundaries parallel to tensile direction under shear stress. With the shear stress increasing, the microcracks extend and coalesce. The fracture of specimens is due to coalescence or shearing between the microcracks.

Keywords: aluminum alloys; tensile shear test; mechanical properties; fracture

1. Introduction

The lightweight automobile meets the requirement of saving energy, protecting the environment, and developing the economy. The aluminum alloys have been used to manufacture the lightweight automobile due to their low density, good plasticity, and high strength/weight ratio [1]. As the main part bearing the weight, the aluminum alloy structure is key to the security and crashworthiness of a vehicle due to its good absorption energy. The forepart can produce lots of rumples and absorb a lot of energy when the automobile collides. Therefore, the latter riding zones can be protected. The equipment of crashworthiness in the front of automobile is a thin-walled tube of aluminum alloy. During the impacting process of the automobile components, the stress states, the damage modes, and the fracture mechanism are different at different locations on the components. In order to accurately perform the FEM calculations and simulations for the components with various damage and fracture models, it is necessary to investigate the deformation, damage, and fracture mechanism of aluminum alloy under various stress states. There are a number of reports on ductile damage and ductile fracture, where the ductile normal fracture (based on the initiation, growth, and coalescence of voids) and shear fracture (based on shear band localization) are addressed as two primary fracture forms for the ductile materials [2-5]. However, most of the stress states are at shear stress states during the impacting process of the automobile components as shown in Fig. 1. There are few reports on mechanical properties and fracture behaviors of 6061 aluminum alloy under shear stress state. This paper studies the mechanical properties and fracture behaviors of 6061 aluminum alloy by means of tensile shear tests under different shear strain rates and *in-situ* tensile shear tests under shear stress state.

2. Method and scheme of experiment

2.1. Experimental material

The experimental material was Al-Mg-Si-Cu series extrusion of a 6061 aluminum alloy (T6) and its microstructure is shown in Fig. 2. Its chemical composition is given in Table 1.

2.2. Specimen preparation

Several kinds of shear specimens were used to investigate the mechanical behaviors of materials by many scholars [6-8]. These specimens were loaded through compression loading and suited for the moderate thick-walled flat, but are not suited for the thin-walled flat. The tensile shear specimen

Corresponding author: ZHU Hao **E-mail:** zhuhao_mallory@163.com

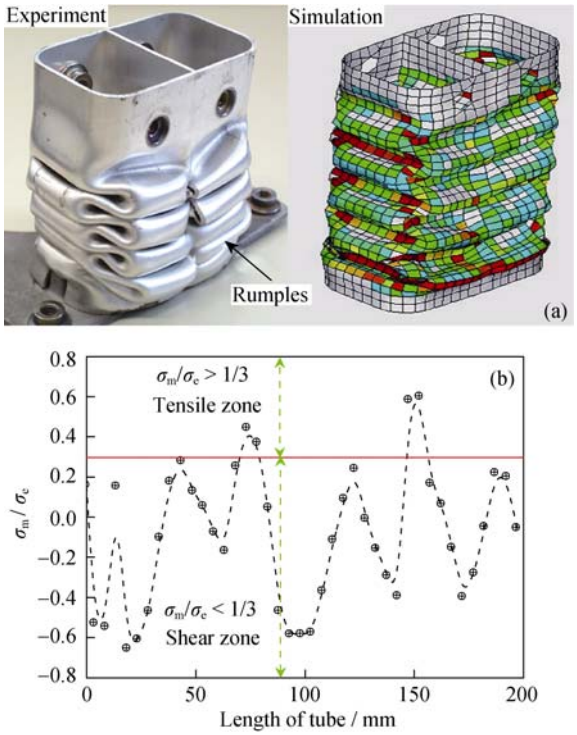

Fig. 1. Rumples and the range of stress triaxiality during the impacting process: (a) rumples of a thin-walled tube during the impacting process; (b) range of stress triaxiality during the impacting process.

Fig. 2. Microstructure of extrusion 6061 aluminum alloy.

Table 1. Composition of the extrusion 6061 aluminum alloy

wt.%

Si	Mg	Fe	Zn	Cu	Mn	Cr
0.69	1.02	0.43	<0.20	0.26	<0.15	0.20

shown in Fig. 3(a) is devised to suit for the thin-walled flat and can be loaded through the tensile loading. Therefore, the mechanical behaviors of 6061 aluminum alloy can be investigated under different shear strain rates. At the same time, the *in-situ* tensile shear specimen shown in Fig. 3(b) is devised and can be used to investigate the process of shear fracture of 6061 aluminum alloy. All the specimens were cut with an electro-discharge machine.

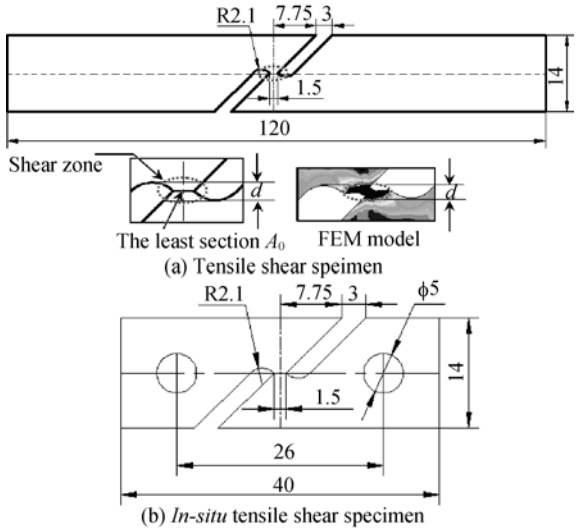

Fig. 3. Two kinds of shear specimens.

2.3. Method of experiment

The tensile tests were performed with the tensile shear specimen shown in Fig. 3(a) by a SHIMADZU AG-10TA test machine at room temperature and the tensile velocity is 1, 30, 120, 360, and 500 mm/min, respectively. The curves of loading-displacement are recorded automatically. The curves of engineering shear stress-strain are gained through the loading divided by the transverse area of the original specimen "A_0" shown in Fig. 3(a) and the displacement divided by the "d" shown in Fig. 3(a). The shear yield stress, shear ultimate stress, and shear fracture strain can be gained by the curves of shear stress-strain. The loading velocity divided by "d" was defined as the average shear strain rate and the shear strain rates were as follows: 0.01, 0.33, 1.33, 4, and 5.56 s^{-1}.

All *in-situ* tensile shear specimens shown in Fig. 3(b) were first polished with SiO_2 paper and then etched with a mixed solvent of 2 mL HF + 3 mL HCL + 35 mL HNO_3 + 190 mL H_2O before testing. The *in-situ* tensile shear tests were carried out in a vacuum chamber by using a calibrated loading stage in a scanning electron microscope (SEM-520). The specimens were slowly step-loaded manually and the crack patterns at various loading steps were recorded by SEM. Crack initiation and propagation processes in conjunction with the applied loads were recorded as well. The loading divided by the smallest transverse area of the original specimen was defined as the shear stress.

3. Results and discussion

3.1. Results of FEM calculation

The distribution of stress triaxiality, normal stress, and shear stress among the smallest transverse area of *in-situ* tensile shear specimens were calculated by a three-dimensional model using the ABAQUS Standard, and the element type of C3D8R was used for simulation. An experimental uniaxial tension true stress-true strain curve of the 6061 aluminum alloy was used as the constitutive equation in the finite element method (FEM) to simulate *in-situ* tensile shear tests. The simulations were performed by using the power-exponent PLASTIC law ($\sigma = K\varepsilon^n$) code of the ABAQUS package. The size of the minimum element was 0.04 mm. The distribution curves of stress triaxiality, the normal stress, and shear stress along the path calculated with ABAQUS are shown in Fig. 4, from which it can be seen that the value of the stress triaxiality achieves the maximum at the root of two notches and decreases subsequently. The value of stress triaxiality achieves the minimum at 0.14 mm from the notch root and remains constant subsequently. Correspondingly, various distributions of normal stress and shear stresses (predicted by FEM) along the path calculated with ABAQUS for tensile shear specimens are shown in Fig. 4(b). These results will be used for analyzing the fracture mechanisms in subsequent sections.

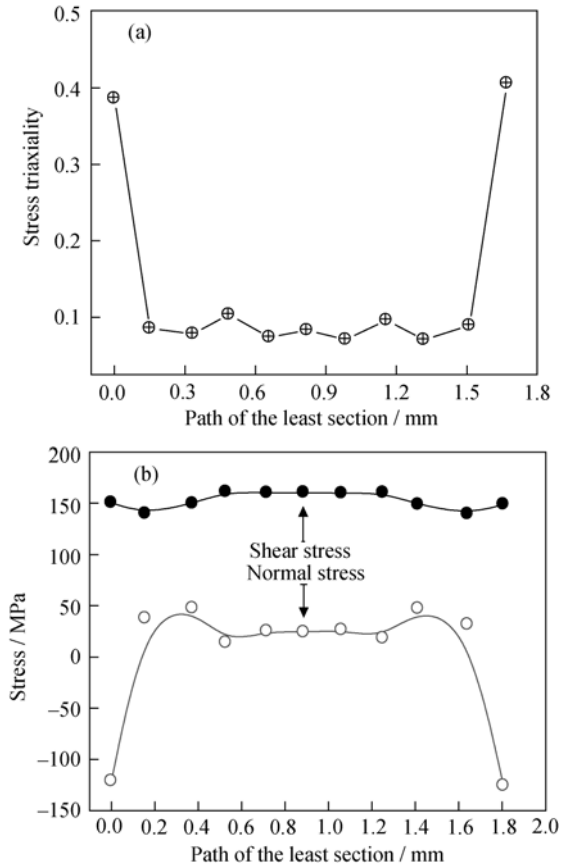

Fig. 4. Distribution of stress triaxiality, normal stress, and shear stress: (a) stress triaxiality; (b) normal stress and shear stress.

3.2. Macroscopic experimental results of tensile shear tests under different shear strain rates

The curves of shear stress-strain under different shear stress are shown in Fig. 5, from which it can be seen that the shear strain rates almost have no influence on the mechanical properties of 6061 aluminum alloy. At the same time, it also proves that the 6061 aluminum alloy is an insensitive material to shear strain rates. However, the shear strain rates have influence on the shear fracture strain of 6061 aluminum alloy, as shown in Fig. 6, which also reflects that the shear fracture strain decreases with the shear strain rates increasing. The shear fracture strain decreases rapidly in the range of 0.01 to 0.33 s^{-1} and almost decreases linearly in the range of 1.33 to 5.56 s^{-1}.

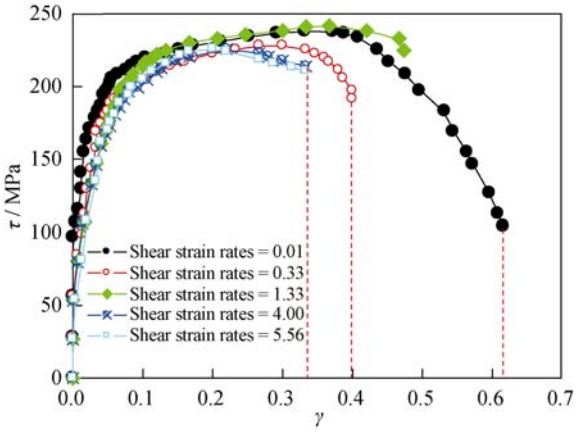

Fig. 5. Curves of shear stress-strain at different shear strain rates.

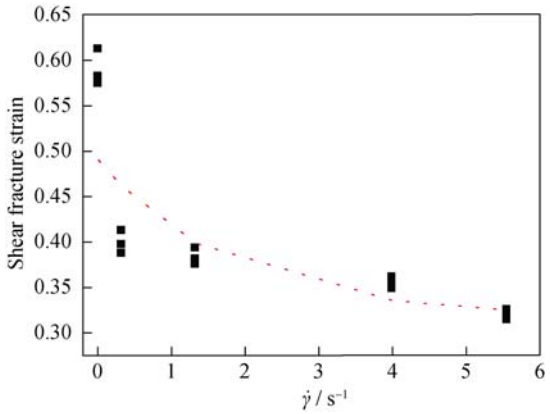

Fig. 6. Relationship between shear fracture strain and shear strain rates.

The tensile shear fracture surfaces are shown in Fig. 7, from which it can be seen that the shear fracture surfaces almost have no difference under different shear strain rates.

In meso-level, the distinct characteristic of shear fracture surfaces is that the fracture surface is made up of many small shear facets compared with the dimples fracture surfaces. There is almost no dimple on the shear fracture surfaces, namely, the voids on the fracture surface do not grow up and coalesce. In theory, the influence factors of fracture surfaces are the stress triaxiality (σ_m/σ_e) and equivalent plastic strain (PEEQ), and the dominant factor is the stress triaxiality. The stress triaxiality controls the size of dimples and equivalent plastic strain controls the depth and direction of dimples. The higher the stress triaxiality is, the bigger the driving force of void growing becomes and the larger the area of circular dimples on the fracture surface tends to be. On the contrary, the less the stress triaxiality is, the bigger the equivalent plastic strain becomes; the less the driving force of voids growing is, the larger the area of the parabola voids becomes. The stress triaxiality of tensile shear specimens under different shear strain rates is close to 0 and the driving force of voids growing is close to 0. Therefore, there are almost no voids on the tensile shear fracture surfaces and the fracture surfaces are made up of many smooth shear facets. To sum up, the shear strain rates have no influence on the tensile shear fracture surfaces.

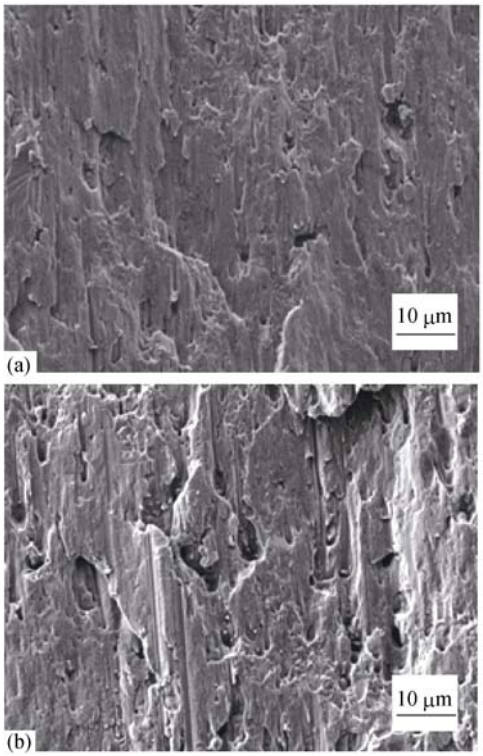

Fig. 7. Tensile shear fracture surfaces of the 6061 aluminum alloy at different shear strain rates: (a) 0.01 s^{-1}; (b) 5.56 s^{-1}.

3.3. Experimental results of *in-situ* tensile shear tests and discussion

Fig. 8 shows the crack initiation, crack propagation, and a general view of the crack extension observed in tensile shear *in-situ* test under different shear stresses. In Fig. 8(b), some slip bands parallel to the loading direction appear when the shear stress reaches 167.54 MPa. It obviously proves that the slip bands are produced under shear stresses. The deformation near root is very serious when the shear stress reaches 167.54 MPa and microcracks are produced at root of notch, far from the root. The main microcrack extends constantly under shear stress, but the shear stress always remains 167.54 MPa, as shown in Fig. 8(c). It proves that the increasing stress due to work hardening exactly makes up the decreasing stress due to microcracks extension. When the shear stress decreases to 165.21 MPa, as shown in Fig. 8(d), a crack of 400 μm in length appears. The angle between the crack and the loading direction is 15°, but it is 0° in theory, which implies that the fracture of *in-situ* tensile shear specimen is not produced completely under shear stress, as proven in Fig. 4.

Based on the above observations and analyses, the fracture mechanism of tensile shear specimen can be summarized as follows. (1) Cracks initiate at grain boundaries by the shear stress, most of which are through the slipping between neighboring grains. (2) Cracks are also extended and connected by the shear stress, either through intergranular boundaries or through transgranular slip band, to keep the general direction in line with the path orientation. (3) The dominant role played by the shear stress is consistent with the calculated results of low stress triaxiality (Fig. 4(a)) and a much higher shear stress relative to the tensile stress distributions (Fig. 4(b)) in the path of the tensile shear specimen.

4. Conclusions

Based on the tensile shear under different strain rates and observations of the *in-situ* tensile shear tests as well as the FEM calculations, the following conclusions can be drawn for the mechanical behaviors and fracture mechanisms of the 6061 aluminum alloy.

(1) The shear strain rate has no effect on the shear yield stress and shear ultimate stress of 6061 aluminum alloy, but it has great effect on shear fracture strain. With shear strain rates increasing, the shear yield stress and shear ultimate stress of 6061 aluminum alloy remain constant basically, but the shear fracture strain decreases obviously. The shear strain rates have no influence on the fracture surfaces.

(2) The grain boundaries of 6061 aluminum alloy are the weakest area and microcracks initiate at the grain boundaries parallel to tensile direction under shear stress. With the shear stress increasing, the microcracks extend and coalesce. The specimens fracture due to coalescence or shearing between the microcracks. The shear stress dominates the crack initia-

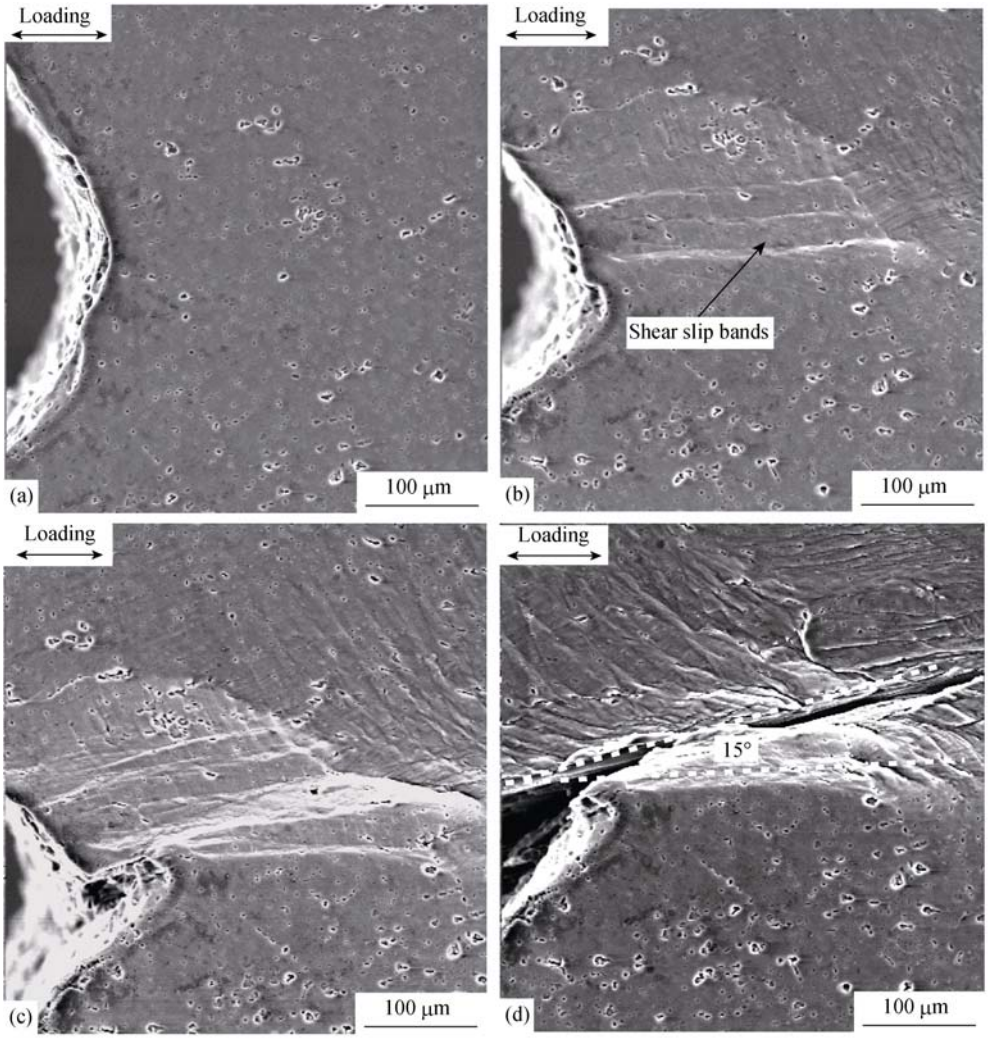

Fig. 8. Surfaces observation of *in-situ* tensile shear specimen: (a) 0 MPa; (b) 167.54 MPa; (c) 167.54 MPa; (d) 165.21 MPa.

tion and the propagation. The initiation and propagation of intergranular cracks are caused by the shear stress. These cracks are connected by the transgranular cracking of the ligaments through the slip bands because of shear stress.

Acknowledgements

This work was financially supported by the Education Department of Hebei Province, China (Nos. 933005 and ZD2010209).

References

[1] Pikett A.K., Pyttel T., and Payen F., Failure prediction for advanced crashworthiness of transportation vehicles, *Int. J. Impact Eng.*, 2004, **30**: 853.

[2] Batra R.C. and Lear M.H., Adiabatic shear banding in plane strain tensile deformations of thermoelastoviscoplastic materials with finite thermal wave speed, *Int. J. Plast.*, 2005, **21**: 1521.

[3] Warren T.L. and Forrestal M.J., Effect of strain hardening and strain-rate sensitivity on the penetration of aluminum targets with spherical-nosed rods, *Int. J. Solid Struct.*, 1998, **35**: 3737.

[4] Zhu H., Zhu L., Chen J.H., and Lv D., Investigation of fracture mechanism of 6063 Al alloy under different stress states, *Int. J. Fract.*, 2007, **146** (3): 159.

[5] Zhu H., Zhu L., Chen J.H., and Lv X.F., The study of deformation and damage mechanism of aluminum alloy (6063) under different stress states, *Rare Met. Mater. Eng.*, 2007, **36** (4): 597.

[6] Yang R.Q., Li S.X., and Zhang Z.F., Cyclic deformation and dynamic compressive properties of copper bicrystals, *Mater. Sci. Eng. A*, 2007, **466** (1-2): 207.

[7] Fleury E. and Ha J.S., Small punch tests to estimate the mechanical properties of steels for steam power plant: I. Mechanical strength, *Int. J. Pressure Vessels Piping*, 1998, **75**: 699.

[8] Finarelli D., Rooding M., and Carsughi F., Small punch tests on austenitic and martensitic steels irradiated in a spallation environment with 530 MeV protons, *J. Nuclear Mater.*, 2004, **328**: 146.